ACADEMIC PRESS

Available online at www.sciencedirect.com

SCIENCE DIRECT®

VIROLOGY

Virology 310 (2003) 298–309

www.elsevier.com/locate/yviro

Defective RNAs of *Citrus tristeza virus* analogous to *Crinivirus* genomic RNAs

Xibing Che,[a] William O. Dawson,[b] and Moshe Bar-Joseph[a,*]

[a] *The S. Tolkowsky Laboratory, Department of Virology, Agricultural Research Organization, the Volcani Center, Bet Dagan, Israel*
[b] *Citrus Research and Education Center, University of Florida, Lake Alfred, FL 33850, USA*

Received 20 November 2002; returned to author for revision 13 December 2002; accepted 15 January 2003

Abstract

The family *Closteroviridae* includes the genera *Closterovirus* and *Ampelovirus* with monopartite genomes and the genus *Crinivirus* with bipartite genomes. Plants infected with the *Closterovirus*, *Citrus tristeza virus* (CTV), often contain one or more populations of defective RNAs (dRNAs). Although most dRNAs are comparatively small (2–5 kb) consisting of the genomic RNA termini with large internal deletions, we recently characterized large dRNAs of ~12 kb that retained the open reading frames (ORFs) 1a plus 1b. These were self-replicating RNAs and appeared to be analogous to the genomic RNA 1 of the bipartite criniviruses. The present report describes the finding of an additional group of large dRNAs (LdRNAs) that retained all or most of the 10 3′ ORFs and appeared to be analogous to genomic RNA 2 of criniviruses. Isolates associated with LdRNAs were found associated with double-recombinant dRNAs (DR-dRNAs) of various sizes (1.7 to 5.1 kb) that comprised the two termini and a noncontiguous internal sequence from ORF2. The genetic and epidemiological implications of the architectural identities of LdRNAs and DR dRNAs and their apparent analogy with the genomic RNA 2 of criniviruses are discussed.

Introduction

Viral RNA recombination, considered a curiosity just two decades ago, now is recognized as a commonly occurring event during replication of many animal and plant viruses, with major effects on the genetic diversity, evolution, and pathological consequences of virus infections (Lai, 1992; van der Most et al., 1992; Simon and Bujarski, 1994; Brian and Spann, 1997; White and Morris, 1999). Studies on the sequences and structural components of viral RNAs that facilitate recombination and take part in the generation of viral defective RNAs (dRNAs) have been advanced by recombinant DNA techniques that have allowed the in vitro construction of helper-dependent (White and Morris, 1994, 1995; Nagy and Simon, 1997, 1998; Nagy and Bujarski, 1998; Bruyere et al., 2000; Mawassi et al., 2000a, 2000b; Knapp et al., 2001; Szittya et al., 2002a) and independent (Penzes et al., 1996; Kim et al., 1997; Satyanarayana et al., 1999) dRNAs derived from different genomic parts of animal and plant viruses. However, despite the range of possible manipulations of artificially constructed dRNA molecules, information on sequences and genomic combinations involved in the fitness, survival, dominance of dRNAs, and their possible involvement in viral evolution is still dependent on the genomic analyses of virus populations that cohabit animal cell cultures and plants.

Citrus tristeza virus (CTV), a *Closterovirus* of the family *Closteroviridae* (Bar-Joseph et al., 1979; Dolja et al., 1994; Agranovsky, 1996; Karasev, 2000) is transmitted vegetatively by budwood during propagation and also by aphids. Trees have been persistently infected with CTV for most or all of their life spans, up to 100 years and vegetative propagation of infected budwood can maintain virus populations for hundreds of years.

The CTV virions are flexuous rods, 2000 nm long and 10–12 nm in diameter with a positive-stranded RNA genome of 19.3 kb, organized into 12 open reading frames (ORFs) (Bar-Joseph et al., 1979, Karasev et al., 1995). The 5′ proximal ORF 1a encodes a 349-kDa polyprotein that

* Corresponding author. Fax: +972-3-9604180.
E-mail address: m6joseph@volcani.agri.gov.il (M. Bar-Joseph).

0042-6822/03/$ – see front matter © 2003 Elsevier Science (USA). All rights reserved.
doi:10.1016/S0042-6822(03)00127-2

includes two cysteine papain proteinase-like domains and methyltransferase- and helicase-like domains. ORF 1b, which is thought to allow the continued translation of the polyprotein by a + 1 frameshift, encodes an RNA-dependent RNA polymerase-like domain (Karasev et al., 1995). The remaining 3′ half of the genome contains a set of 10 ORFs, expressed via 3′ coterminal subgenomic RNAs (sgRNAs) with different 5′ termini (Hilf et al., 1995; Karasev et al., 1997; Yang et al., 1997). Several of the translation products of the CTV sgRNAs were characterized, these include p25 and p27, which constitute the capsid proteins (CPs); p61 and p65, associated with encapsidation and movement; p20, which forms amorphous inclusions; and p23, an RNA binding protein that controls asymmetrical RNA accumulation (Gowda et al., 2000; López et al., 2000; Satyanarayana et al., 2000, 2002). Infected plants produce approximately 30 different subgenomic RNAs in addition to the genomic RNA (Gowda et al., 2001) including relatively large amounts of negative stranded RNAs corresponding to both genomic and 3′ coterminal sgRNAs (Dodds and Bar-Joseph, 1983; Hilf et al., 1995).

Most CTV isolates contain one or more defective RNAs, with molecular sizes ranging from about 2 to 12 kb (Che et al., 2002). The previously characterized CTV dRNAs were composed of the two genomic termini with extensive internal deletions (Mawassi et al., 1995a, 1995b; Yang et al., 1999; Ayllón et al., 1999), plus occasionally a few (~14 nts) nonviral sequences at the junction sites (Mawassi et al., 1995a; Yang et al., 1999). For convenience, we grouped them into classes. Class I consists of 5′ and 3′ termini of various lengths, which were thought to result from nonhomologous recombination. Class II dRNAs retained a common 3′ component containing the 3′-most gene (p23), suggesting that they might arise because of a hot spot of recombination resulting from template switching after the completion of the minus strand of the p23 sgRNA. It could also be that the conservation of the p23 gene provides some competitive or survival advantage for dRNA molecules (Bar-Joseph et al., 1997; Yang et al., 1997). Recently we reported on a new group of large dRNAs (Class III), which retained ORFs 1a and 1b. These large dRNAs designated as L5′dRNAs, contained large 5′ part of CTV genome and were shown to replicate independently in protoplasts, and presumably in plant cells, but could be regularly transmitted by mechanical inoculation to plants and protoplasts demonstrating that they were encapsidated when complemented by a wild-type virus (Che et al., 2002).

In addition the *Closteroviridae* family comprises the mealybug-transmitted *Ampelovirus* genus, with monopartite genomes and the genus *Crinivirus* that consists of whitefly-transmitted viruses with bipartite genomes (Martelli et al., 2002). The type species of crinivirus, *lettuce infectious yellows virus* (LIYV), is composed of two large, positive-sense, single-stranded RNAs: RNA 1 of 8118 nucleotides (nts) includes 3 genes and encodes for proteins that facilitate LIYV RNA replication; RNA 2 of 7193 nts, contains 7 genes, including a 5 gene array that is conserved among all known closteroviruses (Klaassen et al., 1995; Yeh et al., 2000; Karasev, 2000). Unlike the RNAs of LIYV, the RNAs 1 and 2 of *sweet potato chlorotic stunt virus* (SPCSV), a recently characterized crinivirus shares nearly identical 208-nt-long 3′ terminal sequences and the small hydrophobic protein along with an RNAseIII-like protein, which was not found in other closteroviruses, are located in genomic RNA 1 (Kreuze et al., 2002).

A central question concerns how the *Closteroviridae*, with their mono- and bipartite genomes, evolved, and whether there was a role for dRNA molecules in their evolution. Such a possibility could be implied by the apparent analogy between the naturally occurring class III CTV L5′dRNAs (Che et al., 2002) and the genomic RNA 1 of criniviruses. An obvious missing linking was the absence of RNA 2-like dRNAs.

The present report describes the finding of a group of native large dRNAs (LdRNAs) from CTV-infected plants, which retain all or most of the 10 3′ ORFs. These molecules appear to be analogous to RNA 2 of the bipartite criniviruses. We also report on an additional group of double-recombinant dRNAs (DR-dRNAs) that appear to be derivatives of LdRNAs. The genetic implications of the architectural similarities among the LdRNAs, the DR-dRNAs, and the genomic RNAs of criniviruses are discussed.

Results

Detection of dRNAs that retain large 3′ parts of genomic RNA

Northern hybridization of dsRNA-enriched samples (Dodds and Bar-Joseph, 1983) from Israeli CTV isolates (Mawassi et al., 1993; Shalitin et al., 1994), with riboprobes directed toward the termini and three central parts of the genome (Fig. 1A), was used as a means to search for native dRNAs that retained most of the 3′ genes. The reactions of two naturally spreading CTV isolates Gal-T and Ach-T are shown in Fig. 1B, lanes 1 and 2, respectively. In addition to the genomic RNAs, both isolates showed two large dRNA molecules, of about 9.5 and 9.0 kb, designated LdRNA1 and LdRNA2 (Fig. 1B, lanes 2 and 1, indicated by asterisks), respectively, that reacted with probes directed toward the two termini (Fig. 1B, columns *a* and *e*), ORF2 and ORF3+4 (Fig. 1B, *c* and *d*). Neither of these LdRNAs reacted with a probe corresponding to a region of ORF1a, positioned between nts 7422 to 8396 (Fig. 1B, *b*). The hybridization results and the size (~9.0 kb) of the LdRNAs suggested that these molecules had the standard structure of CTV dRNAs, including the genomic termini, but were nevertheless unique in consisting of unusually large 3′ portions.

Isolates Ach-T and Gal-T contained, in addition to LdRNA1 and LdRNA2, respectively, two smaller dRNAs of about 4.5 and 3.2 kb, respectively, that reacted with

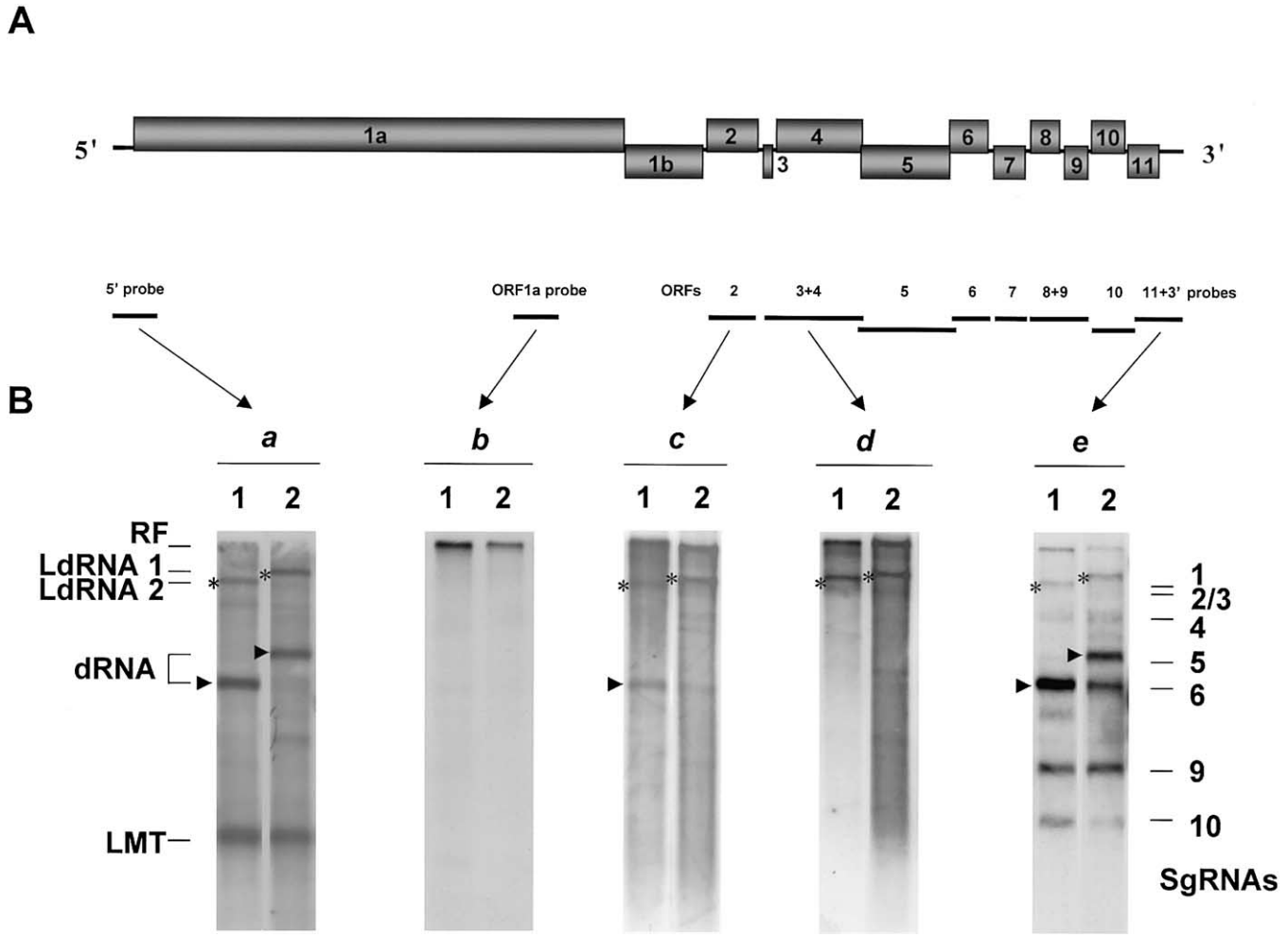

Fig. 1. (A) A diagram of the citrus tristeza virus (CTV) genomic RNA. The ORFs with respective numbers are indicated. The location of the riboprobes that were used in this work and a scale of size are shown under the genomic map. (B) Northern blot hybridizations of dsRNA-enriched extracts from two Alemow plants infected with the CTV isolates Gal-T (lanes 1) and Ach-T (lanes 2) using DIG-labeled riboprobes corresponding to the 5′ 755 nt (*a*), ORF1a 947 nt (*b*), ORF2 (*c*), ORF 3+4 (*d*), and the 3′ 907 nt (*e*). Lanes 1 and 2 in columns *a, c, d,* and *e,* show the large defective RNAs: LdRNA2 and LdRNA1, respectively (indicated by asterisks). Note also the presence of small dRNAs that reacted with some of these riboprobes (marked with arrowheads). The positions of replicative form (RF) RNA, low-molecular-weight 5′ sgRNA (LMT), and 3′ sgRNAs are indicated.

probes directed toward the termini (Fig. 1B, *a* and *e*, indicated by arrowheads). The 3.2-kb dRNA located in Gal-T isolate also hybridized with the ORF2 probe, but not with the probe corresponding to ORFs 3+4 (Fig. 1B, *c* and *d*, lanes 1 indicated by arrowhead).

Graft and mechanical transmission of LdRNAs to plants and protoplasts

The graft transmissibility of LdRNAs was examined by graft inoculation of CTV-free plants. The dsRNAs were extracted 2–3 months postinoculation (mpi) from Alemow plants maintained at 26°C and the dRNAs, as well as the genomic and subgenomic RNAs, were monitored with the 5′ terminus and ORF10 riboprobes. Among the six plants that had been graft-inoculated with chip-buds from the Ach-T-infected source plant, which revealed the presence of LdRNA1 (Fig. 1B, lanes 2), hybridization results consistently showed the presence of LdRNA1 in all graft-inoculated plants (Fig. 2, lanes 1 to 6). Interestingly, three of the graft-inoculated plants contained an additional large dRNA molecule (LdRNA3), of about 9.0 kb (Fig. 2, lanes 3 to 5, marked by arrowheads). Repeated hybridization analyses failed to detect LdRNA3-like molecules directly from the Ach-T source plant (not shown).

A large dRNA, designated as LdRNA4, had a molecular size apparently similar to that of LdRNA3, but was located in a plant designated as no. 29, which was mechanically infected with a mixture of several CTV isolates, including Ach-T, Chl-T, and VT5. This molecule also reacted with riboprobes specific to the 5′ end, ORF2 and ORFs 3+4, and the 3′ end, but not with a probe corresponding to 7422–8329 of ORF1a (not shown), suggesting that it also included a large region of the 3′ part of the CTV genome and was

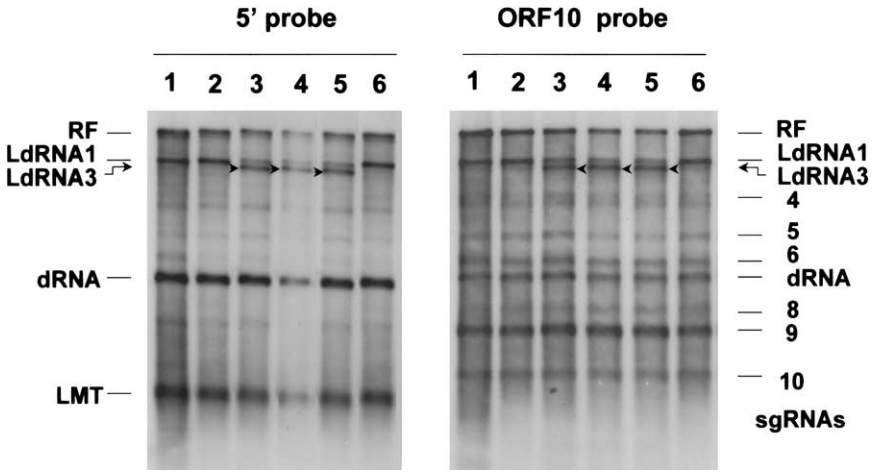

Fig. 2. Northern blot hybridization of dsRNA-enriched extracts from six Alemow plants 3 months after graft inoculation with CTV isolate Ach-T, using riboprobes specific to the 5′ end and to ORF10. The positions of the RF, LdRNA1 (observed in all the tested samples), LdRNA3 (observed in three samples, lanes 3–5, indicated by arrowheads), dRNA, LMT, and 3′ sgRNAs are indicated on the sides.

closely similar in genomic structure to LdRNA1 or LdRNA2.

Northern hybridization of RNA samples from *Nicotiana benthamiana* protoplasts 4 days postinfection (dpi) with fresh tissue extracts of Ach-T-infected plant did not reveal signals of LdRNA molecules. However, low multiplicity replication of LdRNA1 molecules was regularly detected by RT-PCR assays of 4-dpi protoplasts (not shown).

Molecular characterization of the LdRNAs

To investigate the molecular composition of the LdRNAs, we further analyzed them with additional hybridization probes directed toward the 3′ part of the CTV genome, specific to each of the 3′ ORFs including ORFs 3+4, 5, 6, 7, 8+9, and 10 (indicated in Fig. 1A). Fig. 3A shows that LdRNA1 molecules from grafted and the original Ach-T source plants (lanes 1 and 2, respectively) hybridized with all the probes directed toward the 3′ ORFs. The LdRNA3 molecules from grafted samples also reacted with the 3′ ORF probes from ORF3 to ORF10 (Fig. 3A, lanes 1). The LdRNA3 molecules also failed to react with the probe from 7422 to 8396 nts of ORF1a (not shown).

The large sizes of the LdRNAs did not allow their direct RT-PCR amplification with primers specific to their termini. To circumvent this limitation we used the information from the hybridization analyses, which showed that the LdRNAs extended into ORF2 or at least into ORF3, and accordingly we designed seven primers to amplify the junction sites of these molecules. The cDNAs were synthesized from samples containing LdRNA molecules, by using a complementary primer P_1 (Table 1) specific to the CTV 3′ terminus. RT-PCR amplification with primers P_2 (Table 1), corresponding to the CTV extreme 5′ terminus, and antisense-oriented P_3 (Table 1) positioned at the end of ORF1b gave rise to a unique PCR product from LdRNA1 of about 1 kb (Fig. 3B, *a*①). No amplification of LdRNA2 (Fig. 1B, lanes 1) and LdRNA3 (Fig. 3A, lanes 1) was obtained with these primers, suggesting that the resulting DNA fragments contained only the junction site of LdRNA1, which extends into ORF1b. Amplification with primers P_2 and P_4 (within ORF3, Table 1) gave rise to a unique product of 2 kb from a sample of LdRNA1 and one extra band of 1.3 kb from LdRNA3 and a 1.1-kb fragment from LdRNA2 (Fig. 3B, *a*②), indicating that junction sites of LdRNA2 and LdRNA3 were located within the ORF2 of the CTV genome. Primers P_2 and P_5 (within ORF4, Table 1), resulted in three different products: of 3 kb for LdRNA1, of 2.2 kb for LdRNA3, and of 2.0 kb for LdRNA2 (Fig. 3B, *a*③). In addition, PCR amplification with primer P_6 corresponding to nts 652–669 from the 5′ region and P_7 (within ORF5, Table 1) resulted in PCR products of 3.3 kb from LdRNA1, 2.6 kb from LdRNA3, and 2.4 kb from LdRNA2 (Fig. 3B, *a*④). To ensure that the resultant PCR products were obtained from LdRNA templates, similar RT-PCR analyses were performed with dsRNA preparations from two isolates that did not contain LdRNAs. As expected, no corresponding products were obtained with these primer combinations.

The resulting PCR products were isolated and inserted into TA-cloning vector, and sequences of at least two clones from independent RT-PCR assays were determined. The sequences were compared with CTV-VT strain (Mawassi et al., 1996)(GenBank Accession No. 56902). Sequencing of four overlapping PCR fragments derived from LdRNA1 showed a single junction site located at positions 948 and 10682 nt of the genomic RNA (Fig. 3B, *b* (2)). The sequences of LdRNA1 molecules from grafted plants were identical to those of the inoculum source, thus demonstrating regular graft transmission of these large dRNA molecules. The junction sites of LdRNA2 and 3, which were characterized from three overlapping bands for each, consisted of 5′ portions of 948 nt identical to the 5′ region from

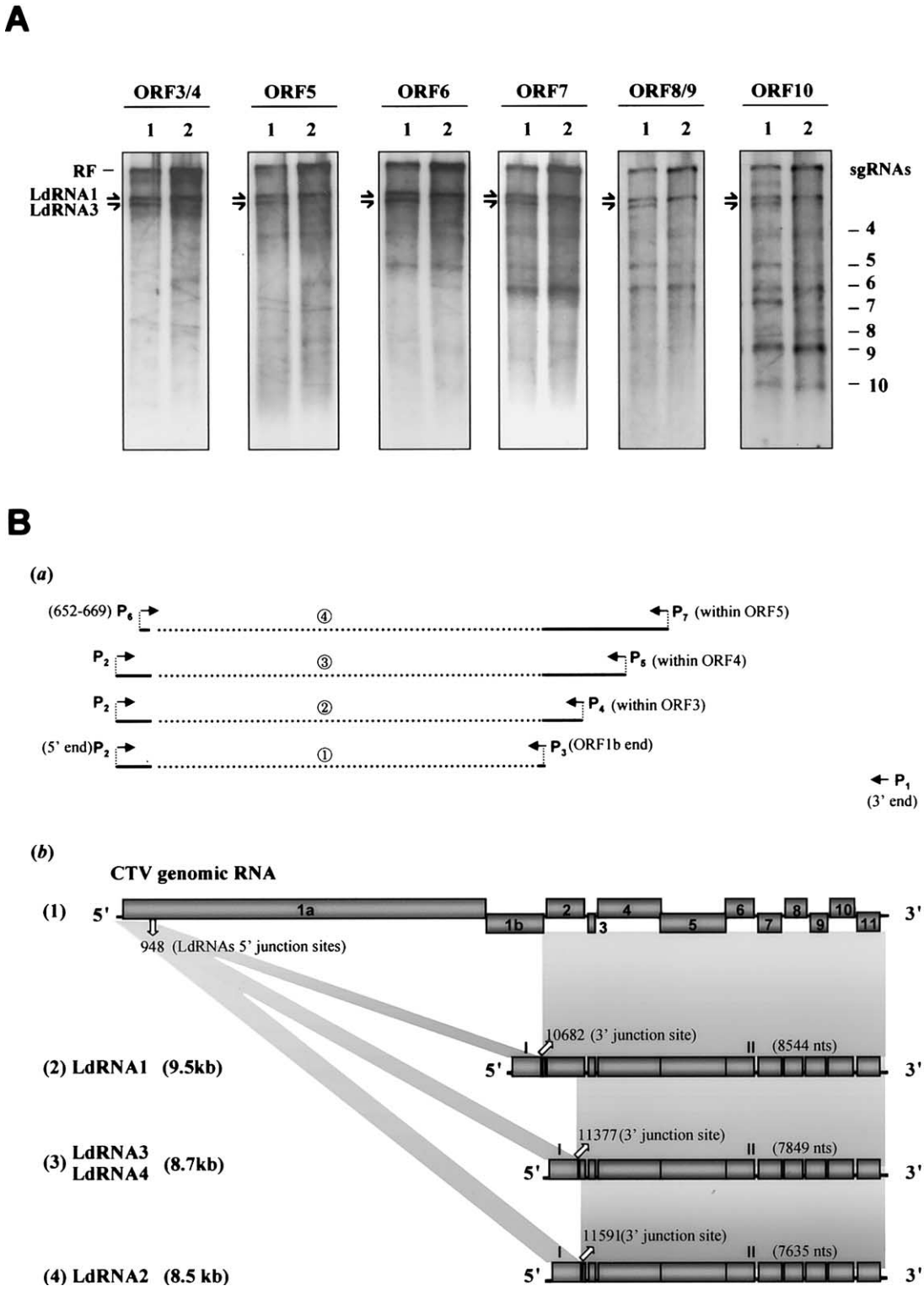

Fig. 3. Northern blot hybridization analysis of dsRNA-enriched extracts from grafted and the original Ach-T source plants, showing LdRNA1 (lanes 1 and 2, respectively) and LdRNA3 which was observed only in samples from grafted plants (lanes 1), using six different riboprobes corresponding to ORF 3+4–ORF10. The dsRNAs corresponding to ORFs 5 to 11 are indicated on the right side of (A). The positions of RF, LdRNA1, and LdRNA3 are shown on the left side of (A). (B) The cloning strategy and sequence organization of LdRNAs. (*a*) The LdRNAs were cloned into four (LdRNA1) or three (LdRNA2, LdRNA3, and LdRNA4, respectively) overlapping fragments (①, ②, ③, and ④ shown as thin lines taken from LdRNA1, as an example); broken lines indicate the position of deletions of the genomic RNA. Arrows indicate the primers P_1 to P_7 and their polarity. Primers are shown at their corresponding location on the genomic RNA (*b*, (1)) and their position is described in parentheses. ORF numbers in genomic RNA (*b*, (1)) are indicated as in Fig. 1A. Diagrammatic representation of the resulting LdRNA sequences (*b*, (2) to (4)). All LdRNAs contain two regions from the CTV genome, an identical 5′ end of 948 nt (region I) and large 3′ parts (region II) of 8544 nt for LdRNA1 (*b*, (2)), 7849 nt for LdRNA3 and LdRNA4 (*b*, (3)), and 7635 nt for LdRNA2 (*b*, (4)). The positions of the rearrangement sites of the various LdRNAs on the CTV genome are shown as open arrows.

Table 1
Oligonucleotide primers used for RT-PCR analyses and DIG–RNA probe preparation

Primer	Polarity	Sequence	Position in VT sequence
P_1	−	ATGGACCTATGTTGGCCCC	19206–19226
P_2	+	AATTTCTCAAATTCACCCGTAC	1–22
P_3	−	GTGTTAGCTCTCAGCGAGAAC	10798–10818
P_4	−	CTCGAGTCGACTGAACCCCGTTTAAACAG	11798–11818
P_5	−	CTCGAGTCGACTCATATATTATCAGATAACTTTCTATC	12688–12713
P_6	+	GGCAAGAATTCTGACCTC	652–669
P_7	−	CTCTCGTCGACATTTCGAGTTGATTC	13785–13764
P_8	−	GCGTTGCAACCTTCGCTA	17334–17351
P_9	−	CCACCGTCGACAAACAAACTAC	15989–16010
P_{10}	−	GGAATGCGGCCGCAATAGATC	16752–16772
P_{11}	−	GTCCGACTTCATAGAGTGTAC	17837–17857
P_{12}	−	GATGGGCACCGGAATGGC	738–755
P_{13}	+	CTCTTTGGACTCATTGAAAGTGTC	7422–7445
P_{14}	−	TAAGAGTCCACAGTGAACACTC	8396–8375
P_{15}	+	AGGTAGTTGAGTCGAGATG	10818–10834
P_{16}	+	CATTGTTATAACGATTTATCGGTGCAC	11893–11919
P_{17}	−	CTGCGGCCGCAATTTCGAGTTG	13758–13780
P_{18}	+	CGACACATATGTCGTCTCATC	13677–13698
P_{19}	−	GCACAGCGGCCGCTCACC	15319–15337
P_{20}	+	CTTACCCTTTCCATATGGCAGG	15256–15277
P_{21}	+	GTCGTTAATTGACGACTCTTG	16043–16064
P_{22}	+	GTCAGGCAGCTTGGG	16723–16737
P_{23}	+	ATGCATATGCGAGCTTACTTTAGT	17695–17712
P_{24}	−	ATATGCGCCACCTCGTTC	18603–18620
P_{25}	+	ATGCCATGGACGATACTAGCGGAC	18325–18343
P_{26}	+	CGCATCTGCAGGTTAATGCCGTCTCTCCG	11597–11614

LdRNA1 and different 3′ parts that started at positions 11591 and 11377 of the CTV genome, respectively (Fig. 3B, *b* (3) and *b* (4)).

A similar strategy was used for characterizing LdRNA4, which is observed in mechanically inoculated Alemow plant no. 29. Sequence characterization of RT-PCR products revealed molecular composition of LdRNA4 identical to that of LdRNA3 (Fig. 3B, *b* (3)). The molecular features of these LdRNAs, including the absence of most of the 5′ part of the CTV genome and the retention of all the 3′ part ORFs, closely resembled those expected for molecules with a genomic composition analogous to crinivirus RNA 2 mol-

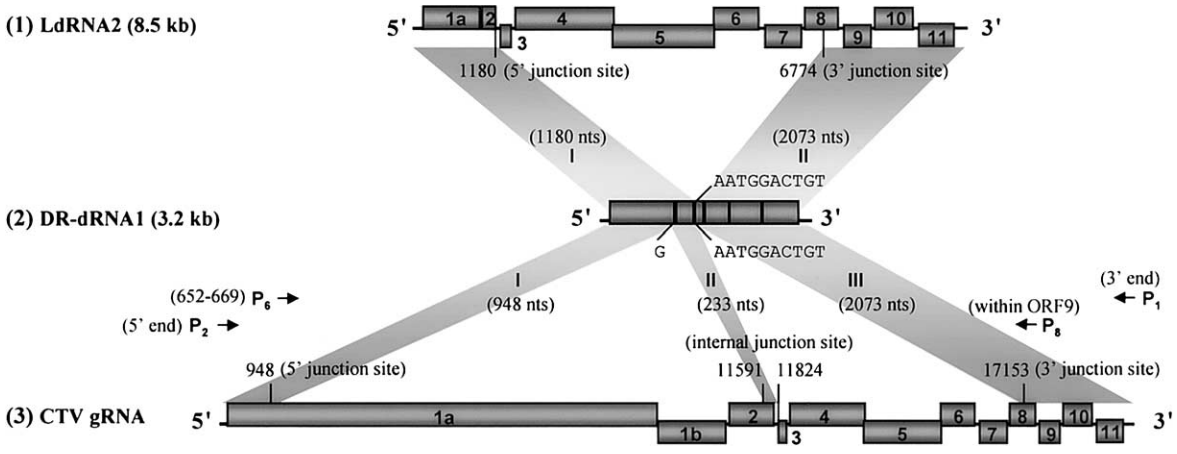

Fig. 4. A diagram showing the structure of DR-dRNA1. The DR-dRNA1 (2) contains two discontinuous regions of LdRNA2 (1): 1180 nt from the 5′ end (region I) and 2073 nt from the 3′ end (region II) of LdRNA2, the junction site between I and II overlap 10 nt; and three discontinuous regions of CTV genome (3): 948 nt from the 5′ end (region I), 153 nt from ORF2, plus the intergenic region of ORFs 2 and 3 and the first 8 nt of ORF3 (233 nt, region II); and ca. 2 kb from the 3′ end of CTV genome (2073 nt, region III), the junction sites between regions I and II and regions II and III contain 1- or 10-nt repeats, respectively. Numbers below LdRNA2 and above CTV genomic RNA boxes indicate the positions of rearrangement sites; lengths of discontinuous regions are indicated by parentheses. Primers used for DR-dRNA1 cloning, their corresponding locations on the genomic RNA and polarity are indicated in parentheses and by arrows. ORFs with numbers are indicated as in Fig. 1A.

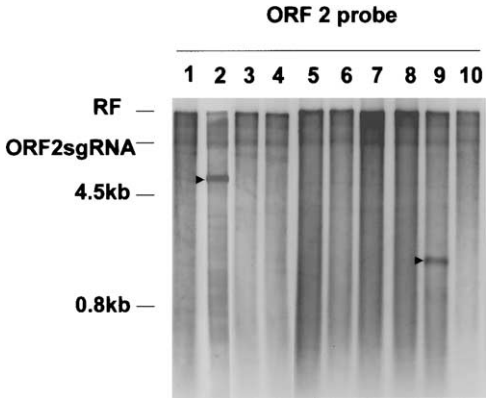

Fig. 5. Northern blot hybridization of dsRNA-enriched extracts from 10 Alemow plants infected with various subisolates of Ach-T (lanes 1–4) and from other Israeli CTV isolates (lanes 5–10) with riboprobe specific to ORF2 of the CTV-VT genome. Two reacting RNAs of ca. 5.0 kb and 1.7-kb RNAs from subisolates Ach-T-33 (lane 2) and MT2 (lane 9), respectively, are indicated by arrowheads. The positions of RF, subgenomic RNA of ORF2, and marker RNAs are given on the left.

ecules. For simplicity, we refer to these LdRNAs as "crini-RNA 2-like dRNAs."

DR-dRNAs associated with large 3′ part dRNAs

In addition to LdRNA2 (Fig. 1B, lanes 1; Fig. 3B, *b* (4)), isolate Gal-T contained a smaller dRNA of about 3.2 kb that reacted with riboprobes directed to the termini and ORF2 but not with the ORF 3+4 probe (Fig. 1B, lanes 1 marked by arrowheads). In order to elucidate the structure of this low-molecular dRNA, two separate RT-PCR reactions were performed on a cDNA template that had been synthesized with the primer P_1, corresponding to the CTV 3′ terminus. Two overlapping fragments of 2.6 and 1.3 kb were obtained by amplification of the resulting cDNA template molecules with primers P_6 and P_1 and primers P_2 and P_8 (positioned as in Fig. 4, Table 1). Because of the large sizes, genomic or large defective RNAs were not expected to be amplified with these primers. Sequencing of the PCR products revealed a molecule of 3243 nt with a composition expected for a DR-dRNA. This molecule, designated as DR-dRNA1, was composed of three noncontiguous regions of CTV genome that included: (I) the 5′-terminal 948 nt; (II) an internal region of 233 nt, corresponding to positions 11591 to 11824 of the genome, which comprised 3′ 153 nt of ORF2, the intergenic region between ORF2 and ORF3, and the first 8 nt from ORF3; and (III) the 3′ 2073 nt that started about 50 nt upstream of the termination codon of ORF8 (Fig. 4, (2) and (3)). The junction sites of DR-dRNA1 between I and II and between II and III showed overlapping sequences of 1 and 10 nt (indicated in Fig. 4), respectively. It should be noted therefore that the length of DR-dRNA1, is 11 nt less than that calculated by summing the lengths of I + II + III.

Alignment of DR-dRNA1 and LdRNA2 from Gal-T isolate suggested that the shorter dRNA was probably derived from a deletion of an internal sequence (nt 1181 to 6773) of LdRNA2 (Fig. 4, (1) and (2)). DR-dRNA1 consisted of two termini from the LdRNA2 genome with 1180 (I) and 2073 (II) nt from the 5′ and 3′ parts, respectively (Fig. 4, (1) and (2)), the junction site between I and II contains a 10-nt overlapping sequence which is identical to that between II and III (Fig. 4). Region I of DR-dRNA1 relative to LdRNA2 was composed of two separate regions, I + II, from CTV genome. The larger amounts of DR-dRNA1 than of LdRNA2 in these samples (Fig. 1B, lanes 1) were in accordance with reports that short dRNAs outcompete larger dRNAs (Szittya et al., 2002b; White and Morris 1994).

The ORF2 probe was used to search for additional DR-dRNA-like molecules among 10 CTV isolates from Israel that did not contain LdRNAs. All samples showed RNA bands corresponding to RF molecules and the ca. 8.3-kb sgRNA of ORF2 (Fig. 5, lanes 1–10). In addition two RNAs of about 5.0 and 1.7 kb were present in one of the four Ach-T subisolates (Ach-T-33) and in a plant infected with naturally spreading MT2 isolate (Fig. 5, lanes 2 and 9, respectively).

To investigate the composition of the ca. 5.0-kb RNA further, the dsRNA-enriched samples from Ach-T-33 infected Alemow plants were hybridized with a panel of probes specific to the genomic RNA 5′ terminus, ORF1a, ORFs 3+4, ORF6, ORF7, and the 3′ terminus, referred to as *a*, *b*, *c*, *d*, *e*, and *f* in Fig. 6A. Only probes specific to 5′ or 3′ termini, ORF6 or ORF7, hybridized with the ca. 5.0-kb RNA (Fig. 6A, *a*, *d*, *e*, and *f*), whereas the ORF1a and ORF

Fig. 6. Diagrammatic representation of DR-dRNA2 and DR-dRNA3. (A) Northern blot hybridization of dsRNA from subisolate Ach-T-33, which contains DR-dRNA2, with riboprobes corresponding to 5′ terminus (*a*), a region of ORF1a (*b*), ORF3+4 (*c*), ORF6 (*d*), ORF7 (*e*), and ORF11 plus the 3′ untranslated region (*f*) from the CTV genome. Hybridization signals of DR-dRNA2 at *a*, *d*, *e*, and *f* are indicated by asterisks. The positions of RF, LMT and 3′ coterminal sgRNA are shown on the two sides. (B) Diagram showing the composition of DR-dRNA2 and DR-dRNA3. Alignment of the three regions of DR-dRNA2 (1) and the CTV genome (2). Note that DR-dRNA2 consists of 948 nt from the 5′ end (region I), 122 nt from the 3′ of ORF2 (region II), and 4053 nt from the 3′ part including an incomplete ORF5 and the entire sequence from ORF6 to the 3′ terminus (region III), Six-nucleotide repeats are shown at the junction site between I and II. Alignment of the three regions of DR-dRNA3 (3) and the CTV genome (2). Region I is identical in all three DR-dRNAs; region II is 232 nt, closely similar to that of DR-dRNA1; and region III is 514 nt. Note the presence of a nonviral 16-nt sequence at the junction site between regions II and III. Numbers below and above CTV genomic RNA boxes show positions of recombination sites. The locations and polarities of primers used for cloning are indicated in parentheses and by arrows, respectively. Lengths of the discontinuous regions are indicated in parentheses. ORFs in the CTV gRNA are indicated as in Fig. 1A. (C) Northern blot hybridization of dsRNA from Alemow plant infected with MT2 isolate, which contains DR-dRNA3, with riboprobes corresponding to 5′ (*a*) and 3′ (*b*) termini and region 11597 to 11818 (*c*) from the CTV genome. All three probes reveal the presence of DR-dRNA3 (indicated by asterisks). The positions of RF, LMT, and 3′ coterminal sgRNA are shown on the side.

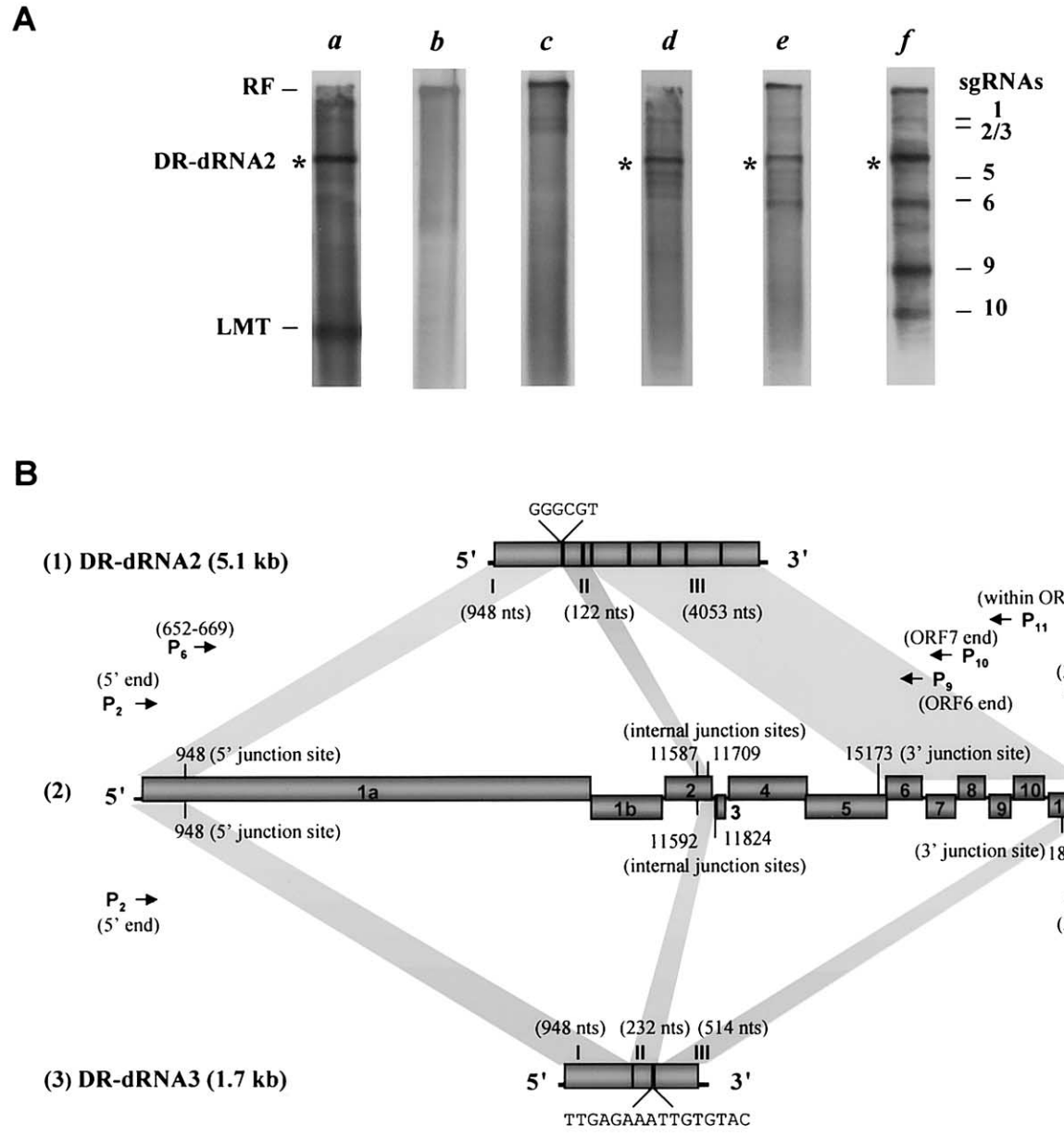
A
a
b
c
d
e
f
RF
DR-dRNA2
LMT
sgRNAs
1
2/3
5
6
9
10
B
(1) DR-dRNA2 (5.1 kb)
GGGCGT
5'
3'
I
II
III
(948 nts)
(122 nts)
(4053 nts)
(within ORF10)
P11
(652-669)
P6
(ORF7 end)
P10
(5' end)
P2
P9
(ORF6 end)
(3' end)
P1
(internal junction sites)
11587 11709
948 (5' junction site)
15173 (3' junction site)
(2)
1a
1b
2
3
4
5
6
7
8
9
10
11
948 (5' junction site)
11592 11824
(internal junction sites)
(3' junction site) 18712
(948 nts) (232 nts) (514 nts)
(3) DR-dRNA3 (1.7 kb)
TTGAGAAATTGTGTAC
C
a
b
c
RF
dRNA
DR-dRNA3
LMT
1
2/3
4
5
6
10
sgRNAs

3+4 probes did not react with the ca. 5.0-kb RNA (Fig. 6A, *b* and *c*). These results suggested that the ca. 5.0-kb dRNA, designated DR-dRNA2, was similar to DR-dRNA1 and that it also consisted of three noncontiguous parts of the genomic RNA, including an internal part derived from ORF2. We analyzed the junction sites of this molecule in three separate reactions with three different oligonucleotide pairs, P_2 and P_9, P_2 and P_{10}, and P_6 and P_{11} (positioned at Fig. 6B, (1), and Table 1), with cDNAs synthesized with primer P_1, corresponding to 3′ end of the genomic RNA. The three overlapping PCR fragments of 1.8 kb from P_2/P_9, 2.5 kb from P_2/P_{10}, and 3.0 kb from P_6/P_{11} were cloned and sequenced. The sequencing data showed that DR-dRNA2 was composed of 948 nt from the 5′ end, 122 nt from ORF2, and 4053 nt from the 3′ end of the CTV genome (Fig. 6B, (1), regions I, II, and III, respectively). A 6-nt repeat, which was found at the junction site of regions I and II, is indicated in Fig. 6B (1).

The 1.7-kb RNA from MT2, designated DR-dRNA3, reacted with the ORF2 probe and riboprobes corresponding to the viral termini in Northern blots (Fig. 5, lane 9 indicated by arrowhead; Fig. 6C, *a* and *b* indicated by asterisks), suggesting that this RNA (DR-dRNA3) was similar to those of DR-dRNAs 1 and 2, and also comprised the two ends of the genome, plus an internal region related to ORF2. To characterize the sequence of DR-dRNA3, primer P_1 was used for cDNA synthesis and the product was amplified directly, with terminal primers P_1/P_2. Sequence characterization of the resulting fragment showed that DR-dRNA3 had a size of 1710 nt; it comprised a 948-nt 5′ end, an internal region which was 1 nt different from DR-dRNA1, and a 514-nt 3′ end, plus a nonviral 16-nt sequence at the junction site of regions II and III (Fig. 6B, (3), regions I, II and III, respectively; 16 nonviral nt are indicated). Hybridization of samples from MT2 with a probe specific to region II of DR-dRNA3 and corresponding to nt 11597 to 11818 of the VT genomic RNA showed, as expected, a strong hybridization signal with the 1.7-kb RNA (Fig. 6C, *c* marked by asterisks).

All three DR-dRNAs, along with their helper virus, were readily observed in samples from graft-inoculated plants by Northern hybridizations with a 5′-specific probe. Sequencing the RT-PCR amplified cDNAs from the plants infected with all three DR-dRNAs confirmed that the DR-dRNAs from graft-inoculated plants were identical with those from the source plants (not shown). However none of the DR-dRNAs were revealed by Northern hybridizations or by RT-PCR in samples of *N. benthamiana* protoplasts inoculated with the sap from the plant infected with Gal-T, Ach-T-33, and MT2 (not shown).

Discussion

Defective RNAs occur in most of the CTV isolates from Israel, Florida, and Spain (Mawassi et al., 1995a, 1995b; Yang et al., 1997, 1999; Ayllón et al., 1999). Understanding of the diversity among CTV dRNAs was extended recently by the finding of a native group of self-replicating large (~12.0 kb) dRNAs (L5′dRNAs) with genetic composition reminiscent of the genomic RNA 1 of bipartite criniviruses (Che et al., 2002). These results raised the question of native dRNAs retaining the 3′ ORFs expected for a dRNA analogous to the genomic RNA 2 of criniviruses (Klaassen et al., 1995; Kreuze et al., 2002). In examining this question, we found among the 18 CTV isolates examined two molecules (LdRNA1 and LdRNA2) of 9492 and 8583 nt, respectively, that showed genetic organization expected for a dRNA analogous to genomic RNA 2 of criniviruses. The larger LdRNA molecule (LdRNA1) consisted of 948 nt from the 5′ end of the CTV genomic RNA and a 3′ part that started 102 nt upstream of the ORF2 start codon. The latter is expected to contain the controller element of p33 and so to allow the synthesis of a complete set of 3′-coterminal mRNAs that express all of these genes (Karasev et al., 1995). The genomic structure of LdRNA2 was essentially similar to that of LdRNA1, with an identical 5′ component and all 3′ ORFs except for ORF2.

Previously we reported that grafting allowed the transmission of both the 2.4- and 4.5-kb dRNAs (Yang et al., 1999) and of the L5′dRNAs, the crini-RNA 1-like dRNAs (Che et al., 2002). In the present work we characterized the sequences from the plants used as inoculum donors and receptors and demonstrated that the large crini-RNA 2-like dRNAs have also been consistently transmitted to new plants. In three of the six plants that had been graft-inoculated with Ach-T, an additional LdRNA (LdRNA3), with a 5′ segment identical to that in LdRNA1, but a 3′ segment 695 nt shorter than that in LdRNA1, was revealed. It is interesting to note that LdRNA3, which was probably generated from a deletion from LdRNA1, was not detected in the donor plant by Northern hybridization or RT-PCR. These results suggest either that LdRNA3 was only erratically present in the donor tissue or that it was generated during the massive increase in virus titers of graft-inoculated Alemow plants.

The finding of LdRNA4 in plant no. 29, which was mechanically infected with a mixture of CTV isolates, including Ach-T, Chl-T, and VT5, indicates that these large and helper-dependent dRNAs can be transmitted mechanically. Further evidence for the infectivity of LdRNA molecules was obtained by sequence analysis of the RT-PCR products from *N. benthamiana* protoplasts, 4 dpi, inoculated with sap from an Ach-T-infected plant. Both observations suggest that the dRNAs can be encapsidated. The low concentrations of LdRNA1 molecules in infected protoplasts, as indicated by the absence of a visible hybridization signal, indicate a low probability of double infection of protoplasts by LdRNAs and full-length helper virus.

Two CTV isolates of Gal-T and MT2 and a subisolate of Ach-T-33 contained major populations of DR-dRNAs of

similar configuration including three noncontiguous genomic regions. DR-dRNA1, DR-dRNA2, and DR-dRNA3 genomes, of 3.2, 5.1, and 1.7 kb, respectively, consisted of an identical CTV 5′ end, the small internal segments of 122 to 233 nt from the end of ORF 2 (DR-dRNA2) plus the beginning of ORF3 (DR-dRNA1 and DR-dRNA3), and the 3′ termini that differed considerably from one another, at 2073, 4053, and 514 nt (in DR-dRNA1, 2, and 3, respectively). The similarities in the 5′ regions (948 nt) of LdRNAs and DR-dRNAs favor a lineage relationship that probably started with a parent similar to LdRNA1 followed by a succession of deletions that conserved the 5′ region and evolved into smaller dRNAs. The finding of a close relationship between LdRNA2 and DR-dRNA1 and their presence in the same Gal-T-infected plant strongly support this hypothesis. An alternative possibility is that the identical 5′ region resulted independently due to a hot spot of recombination and/or preferential selection. De novo generation of a DR-dRNA was reported recently in LIYV-infected protoplasts (Rubio et al., 2002).

In the present work we demonstrated the presence of dRNAs of a monopartite virus analogous to the genomic RNAs of a related bipartite genus within the same family. The crini-RNA 1-like and crini-RNA 2-like LdRNA molecules have not so far been found to naturally coinfect the same citrus plants in Israel. However, CTV epidemics have occurred only during the last two decades (Bar-Joseph et al., 1989). It will be interesting to search for coinfection with the two types of LdRNAs in other geographic areas where virus-infected trees have persisted for centuries.

Materials and methods

Virus sources and propagation

The biological, serological, and genomic characteristics of CTV isolates Ach-T, Chl-T, and VT were described previously (Shalitin et al., 1994; Mawassi et al., 1993, 1996). The Ach-T subisolates were collected in 1980 from a grove of massively infected, symptomless sweet orange trees (cv. Shamouti) grafted on sour orange. Isolate Gal-T was collected in 1988, from a cv. star ruby grapefruit (*Citrus paradisi*) that showed decline and stem pitting, and MT2 was collected in 1992 from a naturally infected Meyer lemon plant. The CTV isolates were passaged annually and propagated in Alemow (*C. macrophylla*) seedlings. Infected plants were maintained in insect-free screenhouses or glasshouses with temperatures ranging between 15 and 35°C.

Mechanical inoculation of Citrus plants and N. benthamiana protoplasts

Fresh bark tissues from Alemow plants infected with the VT, Chl-T, Ach-T, MT2, or Gal-T CTV isolates from Israel were mixed and 2-g batches were pulverized in liquid nitrogen and extracted by shaking on ice with 40 mM phosphate buffer, pH 8.2 (1:5 g/ml) for 15 min. The slurry was squeezed through cheesecloth and kimwipes paper and centrifuged for 10 min at 1000*g;* after the removal of 0.5 ml of supernatant solution (S1) the virus was precipitated from the rest of the supernatant by adding PEG and NaCl to 6% and 0.1 N, respectively, and incubated at 4°C for 1 h. The solution was centrifuged for 15 min at 10,000*g*, and the pellet was resuspended in S1 and used for slash inoculation of stems of 12- to 18-month-old Alemow seedlings according to Garnsey (1977), with slight modifications as described by Satyanarayana et al. (2001).

Protoplasts from expanded leaves of *N. benthamiana* were prepared according to Navas-Castillo et al. (1997). The cells were inoculated with freshly extracted sap from bark tissue of infected Alemow plants according to Mawassi et al. (2000b).

RNA extraction and riboprobe preparation for Northern blotting

Bark tissue of infected plants was used to obtain RNA extracts, which were enriched in dsRNA molecules by passing through a single CF11 column according to Dodds and Bar-Joseph (1983). Total nucleic acids was prepared from protoplasts according to Satyanarayana et al. (1999); briefly, protoplasts were pelleted by centrifugation, dissolved in 400 μl of lysis buffer (50 mM Tris–HCl, 100 mM NaCl, 10 mM EDTA, 2% SDS, pH 9.0), followed by two successive phenol–chloroform extractions and ethanol precipitations. The RNAs were separated by electrophoresis in a formamide–formaldehyde denaturing 1.1% agarose gel in MOPS buffer and transferred to Hybond N+ membranes according to Lewandowski and Dawson (1998). Detection of the membranes with nonradioactive DIG-labeled riboprobes was carried out according to Lewandowski and Dawson (1998). The following riboprobes were prepared from selected regions of the CTV gRNA: (i) the 5′ probe which includes 1–755 nt from the 5′ terminus; (ii) the ORF1a probe, including a region of ORF1a from 7422–7445 nt; (iii) probes of ORF2, ORF 3+4, ORF5, ORF6, ORF7, ORF 8+9, and ORF10 covering entire ORFs of the respective numbers; (iv) ORF11 plus 3′ probe, which includes a full-size ORF11 and the 3′UTR of gRNA. The fragments were synthesized by RT-PCR using dsRNA as template and CTV-specific primers (Table 1) inserted into pDrive Cloning Vector (QIAGEN) and used to synthesize positive- or negative-stranded-RNA-specific probes by using T7– or SP6–RNA polymerase.

RT-PCR and molecular analyses

RNA preparations enriched in dsRNA molecules from plants and protoplasts were denaturated with methyl mercury hydroxide, and the regions surrounding the junction sites were amplified by RT-PCR with the primers listed in

Table 1. The resulting PCR products were electrophoresed on 2% agarose gel, isolated with GeneClean, cloned in the AT vector, pDrive Cloning Vector (QIAGEN), according to the manufacturers instructions, and sequenced at a commercial facility (MBC, Rehovot, Israel). The sequence and nucleotide numbering are according to the CTV-VT strain described previously by Mawassi et al. (1996) (GenBank Accession Number U56902). The sequences of seven of the dRNAs described in this paper were deposited in GenBank.

Acknowledgments

The US–Israel Binational Agricultural Research and Development Fund (BARD) supported this work. The authors thank Dr. Munir Mawassi for valuable discussions and Mr. Y. Ben-Shalom for technical assistance.

References

Agranovsky, A.A., 1996. Principles of molecular organization, expression and evolution of closteroviruses: over the barriers. Adv. Virus Res. 47, 119–158.

Ayllón, M.A., Lopez, C., Navas-Castillo, J., Mawassi, M., Dawson, W.O., Guerri, J., Flores, R., Moreno, P., 1999. New defective RNAs from citrus tristeza virus: evidence for a replicase-driven template switching mechanism in their generation. J. Gen. Virol. 80, 817–821.

Bar-Joseph, M., Garnsey, S.M., Gonsalves, D., 1979. The closteroviruses: a distinct group of elongated plant viruses. Adv. Virus Res. 25, 93–168.

Bar-Joseph, M., Marcus, R., Lee, R.F., 1989. The continuous challenge of citrus tristeza virus control. Annu. Rev. Phytopathol. 27, 291–361.

Bar-Joseph, M., Yang, G., Gafny, R., Mawassi, M., 1997. Subgenomic RNAs: the possible building blocks for modular recombination of Closteroviridae genome. Semin. Virol. 8, 113–119.

Brian, D.A., Spann, J.M., 1997. Recombination and coronavirus defective interfering RNAs. Semin. Virol. 8, 101–111.

Bruyere, A., Wantroba, M., Flasinski, S., Dzianott, A., Bujarski, J.J., 2000. Frequent homologous recombination events between molecules of one RNA component in a multipartite RNA virus. J. Virol. 74, 4214–4219.

Che, X., Mawassi, M., Bar-Joseph, M., 2002. A novel class of large and infectious defective RNAs of citrus tristeza virus. Virology 298, 133–145.

Dodds, J.A., Bar-Joseph, M., 1983. Double-stranded RNA from plants infected with closteroviruses. Phytopathology 73, 419–423.

Dolja, V.V., Karasev, A.V., Koonin, E.V., 1994. Molecular biology and evolution of closteroviruses: sophisticated build-up of large RNA genomes. Annu. Rev. Phytopathol. 32, 261–285.

Garnsey, S.M., Gonsalves, D., Purcifull, D.E., 1997. Mechanical transmission of citrus tristeza virus. Phytopathology 73, 419–423.

Gowda, S., Satyanarayana, T., Ayllón, M.A., Albiach-Marti, M.R., Mawassi, M., Rabindran, S., Garnesy, S.M., Dawson, W.O., 2001. Characterization of the cis-acting elements controlling subgenomic mRNAs of citrus tristeza virus: production of positive- and negative-stranded 3′-terminal and positive-stranded 5′-terminal RNAs. Virology 286, 134–151.

Gowda, S., Satyanarayana, T., Davis, C.L., Navas-Castillo, J., Albiach-Marti, M.R., Mawassi, M., Valkov, N., Bar-Joseph, M., Moreno, P., Dawson, W.O., 2000. The p20 gene product of citrus tristeza virus accumulates in the amorphous inclusion bodies. Virology 274, 246–254.

Hilf, M.E., Karasev, A.V., Pappu, H.R., Gumpf, D.J., Niblett, C.L., Garnsey, S.M., 1995. Characterization of citrus tristeza virus subgenomic RNAs in infected tissue. Virology 208, 576–582.

Karasev, A.V., 2000. Genetic diversity and evolution of closterovirus. Annu. Rev. Phytopathol. 38, 293–324.

Karasev, A.V., Boyko, V.P., Gowda, S., Nikolaeva, O.V., Hilf, M.E., Koonin, E.V., Niblett, C., Cline, K.C., Gumpf, D.J., Lee, R.F., Garnsey, S.M., Lewandowski, D.J., Dawson, W.O., 1995. Complete sequence of the citrus tristeza virus RNA genome. Virology 208, 511–520.

Karasev, A.V., Hilf, M.E., Garnsey, S.M., Dawson, W.O., 1997. Transcription strategy of closteroviruses: mapping the 5′ termini of the citrus tristeza virus subgenomic RNAs. J. Virol. 71, 6233–6236.

Kim, K.H., Narayanan, K., Makino, S., 1997. Assembled coronavirus from complementation of two defective interfering RNAs. J. Virol. 69, 2313–2321.

Klaassen, V.A., Boeshore, M.L., Koonin, E.V., Tian, T., Falk, B.W., 1995. Genome structure and phylogenetic analysis of lettuce infectious yellows virus, a whitefly-transmitted, bipartite closterovirus. Virology 208, 99–110.

Knapp, E., Dawson, W.O., Lewandowski, D.J., 2001. Conundrum of the lack of defective RNAs (dRNAs) associated with tobamovirus infections: dRNAs that can move are not replicated by the wild-type virus; dRNAs that are replicated by the wild-type virus do not move. J. Virol. 75, 5518–5525.

Kreuze, J.F., Savenkov, E.I., Valkonen, J.P., 2002. Complete genome sequence and analyses of the subgenomic RNAs of sweet potato chlorotic stunt virus reveal several new features for the genus *Crinivirus*. J. Virol. 76, 9260–9270.

Lai, M.M.C., 1992. RNA recombination in animal and plant viruses. Microbiol. Rev. 56, 61–79.

Lewandowski, D.J., Dawson, W.O., 1998. Deletion of the internal sequences results in tobacco mosaic virus defective RNAs that accumulate to high levels without interfering with replication of the helper virus. Virology 251, 427–437.

López, C., Navas-Castillo, J., Gowda, S., Moreno, P., Flores, R., 2000. The 23-kDa protein coded by the 3′-terminal gene of citrus tristeza virus is an RNA-binding protein. Virology 269, 462–470.

Martelli, G.P., Agranowsky, A.A., Boscia, D., Bar-Joseph, M., Coutts, R.H.A., Gonslaves, D., Minafra, A., Wisler, G.C., Candresse, T., Dolja, V.V., Falk, B.W., Jlkmann, W., Karasev, A.V., Namba, S., Vetten, H.J., Yoshikava, N., 2002. The family Closteroviridae revised. Arch. Virol. 147, 239–244.

Mawassi, M., Gafny, R., Bar-Joseph, M., 1993. Nucleotide sequence of the coat protein gene of citrus tristeza virus: comparison of biologically diverse isolates collected in Israel. Virus Genes 7, 265–275.

Mawassi, M., Karasev, A.V., Mietkiewska, E., Gafny, R., Lee, R.F., Dawson, W.O., Bar-Joseph, M., 1995a. Defective RNA molecules associated with the citrus tristeza virus. Virology 208, 383–387.

Mawassi, M., Mietkiewska, E., Gofman, R., Yang, G., Bar-Joseph, M., 1996. Unusual sequence relationships between two isolates of citrus tristeza virus. J. Gen. Virol. 77, 2359–2364.

Mawassi, M., Mietkiewska, E., Hilf, M.E., Ashoulin, L., Karasev, A.V., Gafny, R., Lee, R.F., Garnsey, S.M., Dawson, W.O., Bar-Joseph, M., 1995b. Multiple species of defective RNAs in plants infected with citrus tristeza virus. Virology 214, 264–268.

Mawassi, M., Satyanarayana, T., Albiach-Marti, M.R., Gowda, S., Ayllón, M.A., Robertson, C., Dawson, W.O., 2000a. The fitness of citrus tristeza virus defective RNAs is affected by the lengths of their 5′- and 3′-termini and by the coding capacity. Virology 275, 42–56.

Mawassi, M., Satyanarayana, T., Gowda, S., Albiach-Marti, M.R., Robertson, C., Dawson, W.O., 2000b. Replication of heterologous combinations of helper and defective RNA of citrus tristeza virus. Virology 267, 360–369.

Nagy, P.D., Bujarski, J.J., 1998. Silencing homologous RNA recombination hot spots with GC-rich sequences in brome mosaic virus. J. Virol. 72, 1122–1130.

Nagy, P.D., Simon, A.E., 1997. New insights into the mechanisms of RNA recombination. Virology 235, 1–9.

Nagy, P.D., Simon, A.E., 1998. In vitro characterization of late steps of RNA recombination in turnip crinkle virus. II. The role of the priming stem and flanking sequences. Virology 249, 393–405.

Navas-Castillo, J., Albiach-Marti, M.R., Gowda, S., Hilf, M.E., Garnsey, S.M., Dawson, W.O., 1997. Kinetics of accumulation of citrus tristeza virus RNAs. Virology 228, 92–97.

Penzes, Z., Wroe, C., Brown, T.D., Britton, P., Cavanagh, D., 1996. Replication and packaging of coronavirus infectious bronchitis virus defective RNAs lacking a long open reading frame. J. Virol. 70, 8660–8668.

Rubio, L., Tian, T., Yeh, H.H., Livieratos, Y., Falk, B.W., 2002. De novo generation of lettuce infectious yellows virus defective RNAs in protoplast. Mol. Plant Pathol. 3, 321–327.

Satyanarayana, T., Bar-Joseph, M., Mawassi, M., Albiach-Marti, M.R., Ayllón, M.A., Gowda, S., Hilf, M.E., Moreno, P., Garnsey, S.M., Dawson, W.O., 2001. Amplification of citrus tristeza virus from a cDNA clone and infection of citrus trees. Virology 280, 87–96.

Satyanarayana, T., Gowda, S., Ayllón, M.A., Albiach-Marti, M.R., Rabindran, S., Dawson, W.O., 2002. The p23 protein of citrus tristeza virus controls asymmetrical RNA accumulation. J. Virol. 76, 473–483.

Satyanarayana, T., Gowda, S., Boyko, V.P., Albiach-Marti, M.R., Mawassi, M., Navas-Castillo, J., Karasev, A.V., Dolja, V., Hilf, M.E., Lewandowski, D.J., Moreno, P., Bar-Joseph, M., Garnsey, S.M., Dawson, W.O., 1999. An engineered closterovirus RNA replicon and analysis of heterologous terminal sequences for replication. Proc. Natl. Acad. Sci. USA 96, 7433–7438.

Satyanarayana, T., Gowda, S., Mawassi, M., Albiach-Marti, M.R., Ayllón, M.A., Robertson, C., Garnsey, S.M., Dawson, W.O., 2000. Closterovirus encoded HSP70 homolog and p61 in addition to both coat proteins function in efficient virion assembly. Virology 278, 1253–1265.

Shalitin, D., Mawassi, M., Gafny, R., Leitner, O., Cabilly, S., Bar-Joseph, M., 1994. Serological characterization of citrus tristeza virus isolates from Israel. Ann. Appl. Biol. 125, 105–113.

Simon, A.E., Bujarski, J.J., 1994. RNA-RNA recombination and evolution in virus-infected plants. Annu. Rev. Phytopathol. 32, 337–362.

Szittya, G., Molnar, A., Silhavy, D., Hornyik, C., Burgyan, J., 2002a. Short defective interfering RNAs of tombusviruses are not targeted but trigger posttranscriptional gene silencing against their helper virus. Plant Cell 14, 359–372.

Szittya, G., Silhavy, D., Dalmay, T., Burgyan, J., 2002b. Size-dependent cell-to-cell movement of defective interfering RNAs of Cymbidium ringspot virus. J. Gen. Virol. 83, 1505–1510.

van der Most, R.G., Heijnen, L., Spaan, W.J.M., Degroot, R.J., 1992. Homologous RNA recombination allows efficient introduction of site-specific mutations into the genome of coronavirus MHV-A59 via synthetic co-replicating RNAs. Nucleic Acids Res. 20, 3375–3381.

White, K.A., Morris, T.J., 1994. Nonhomologous RNA recombination in tombusviruses: generation and evolution of defective interfering RNAs by stepwise deletions. J. Virol. 68, 14–24.

White, K.A., Morris, T.J., 1995. RNA determinants of junction site selection in RNA virus recombinants and defective interfering RNAs. RNA 1, 1029–1040.

White, K.A., Morris, T.J., 1999. Defective and defective interfering RNAs of monopartite plus-strand RNA plant viruses. Curr. Top. Microbiol. Immunol. 239, 1–17.

Yang, G., Che, X., Gofman, R., Ben-Shalom, Y., Piestun, D., Gafny, R., Mawassi, M., Bar-Joseph, M., 1999. D-RNA molecules associated with sub-isolates of the VT strain of citrus tristeza virus which induce different seedling-yellows reactions. Virus Genes 19, 5–13.

Yang, G., Mawassi, M., Gofman, R., Gafny, R., Bar-Joseph, M., 1997. The involvement of a subgenomic mRNA in the generation of a variable population of defective citrus tristeza virus molecules. J. Virol. 71, 9800–9802.

Yeh, H.H., Tian, T., Rubio, L., Crawford, B., Falk, B.W., 2000. Asynchronous accumulation of lettuce infectious yellows virus RNAs 1 and 2 and identification of an RNA 1 trans enhancer of RNA 2 accumulation. J. Virol. 74, 5762–5768.